06

III

ERTS

RECEIVED
NASA STI FACILITY
ACQ. BR. NonExcl
APR 09 1976
DCAF# 004669
1 2 3 4 5

STUDY OF MESOSCALE PHENOMENA, WINTERMONSOON CLOUDS AND SNOW AREA BASED ON LANDSAT DATA

E76-10261
CR-146633

(NASA Hq Reg No 022, GSFC FO 427)

ORIGINAL CONTAINS COLOR ILLUSTRATIONS

Original photography may be purchased from:
EROS Data Center
10th and Dakota Avenue
Sioux Falls, SD 57198

by

KIYOSHI TSUCHIYA

NATIONAL SPACE DEVELOPMENT AGENCY OF JAPAN

2-4-1, Hamamatsu-cho, Minato-ku, Tokyo, 105, JAPAN

JAN 1976

(E76-10261) STUDY OF MESOSCALE PHENOMENA, WINTER MONSOON CLOUDS AND SNOW AREA BASED ON LANDSAT DATA (National Space Development Agency) 33 p HC $4.00 CSCL 08L

N76-21631

Unclas
G3/43 00261

1022A

RECEIVED
MAR 01 1976
SIS/902.6

CONTENTS

STUDY OF MESOSCALE PHENOMENA, WINTER MONSOON CLOUDS AND SNOW COVER AREA BASED ON LANDSAT DATA*

Kiyoshi Tsuchiya

National Space Development Agency of Japan. 2-4-1, Hamamatsu-cho, Minato-ku, Tokyo, Japan

ABSTRACT

Detailed analyses of the clouds in LANDSAT pictures are made in an attempt to study mesoscale phenomena in meteorology with a special emphasis on winter monsoon clouds. The findings are summarized as follows.

A longitudinal clouds street which appears as a continuous cloud in a meteorological satellite picture is found to be consisted of many cloud elements and narrow transversal banded clouds and the ratio of cloud street width to the wave length of the transversal banded cloud ranges from 3 to 5.

Mountain lee wave clouds appear mostly during cold season in and around Japan. The wave length obtained from LANDSAT pictures ranges from 8 to 22 kms. It is also found that the mountain lee wave of different wave length frequently exists in a narrow area. It is also found that LANDSAT pictures are extremely useful in delineating snowcover area, however it is difficult to get snow depth.

A thin cirrus can be detected if the pictures of different spectrum are used. The global albedoe of an urban area and a mountainous area with thick vegetation in the spectral range of 0.8 - 1.1 μm is almost equal in the value with the following characteristics: in short wave spectrum the former has larger value than the latter while in long wave spectrum the opposit relationship holds. It is found that in the vicinity of a clear air turbulence a particular type of cirrus is recognized. Sea fog in LANDSAT picture reveals existence of approximately 1 km wave length motion.

1. INTRODUCTION

LANDSAT data with a spatial resolution of approximately 80 meters with responsibity in 4 different spectra are ideal for the study of mesoscale meteorological cloud features which are too large for aerial photographs yet too small for those of meteorological satellite pictures.

---

* NASA Hq. Reg. No. 022, GSFC ID FO 427.

In this report the findings through the analyses of LANDSAT data, i. e. (1) mesoscale features of clouds formed associataed with cold air outbreak, (2) mountain lee wave clouds, (3) meso-high, (4) snow cover, (5) thin cirrus and radiation characteristics, (6) clear air turbulence, (7) sea fog, are discussed.

Since the several independent subjects are covered in this report instead of stating introduction on whole subjects in the beginning it is decided to give a short introductory remark in the beginning of each subject. Throughout the paper radio soundings will be referred often, therefore the location, name and international station numbers of aerological stations are plotted on a topographical map and is shown in Fig. 1.

2. RESOLUTION OF A PICTURE AND CLOUD APPEARANCE

In the interpretation of pictures taken from space, resolution of pictures must always be considered. An example of difference in appearance of clouds due to the difference of resolution is shown in Fig. 2 and Fig. 3 which are taken almost simultaneously from space the former by meteorological satellite ESSA 8 and the latter by LANDSAT-1.

Fig. 2 shows winter monsoon cloud over northern Japan and her surroundings while Fig. 3, LANDSAT picture covers very narrow area indicated by an arrow in Fig. 2. Latitudinal and longitudinal lines in Fig. 2 are drawn every 2 degrees while in Fig. 3 they are drawn every half a degree therefore the area of LANDSAT picture corresponds to just 1. 5 of the rectangle made by latitudinal and longitudinal lines in Fig. 2. Comparing these two figures it is easily seen that the clouds which have an appearance of stratus in Fig. 2 are composed of small cumuli.

When satellite pictures first became available there were many discussions on the width to height ratio and also structure of covective clouds (i.e. Kreuger and Fritz, 1962, Priestrey, 1961) since the value was nearly 10 times as large as that found by Bénard (1936) and accepted until that time. It is considered that the value obtained from meteorological satellite pictures at that time could not resolve detailed structure of clouds. Thus it has become necessary to revise or modify a part of the results obtained from old meteorological satellite pictures at least mesoscale feature of clouds is concerned.

3. WINTER MONSOON CLOUDS

During cold season, a well developed anticyclone develops over Asiatic continent and Japanese weather is greatly influenced by winter monsoon caused by the persisted anticyclone over the continent. Associated with a strong cold air outbreak from the continent an active formation fof convective clouds takes place over the neighboring sea especially over the warm ocean current. Asai (1964, 1967) made the analyses of the winter monsoon clouds off the coast of Hokuriku District based on aerial photographs while present author (1966, 1967, 1969, 1974) made the analyses of the clouds revealed

PRECEDING PAGE BLANK NOT FILMED

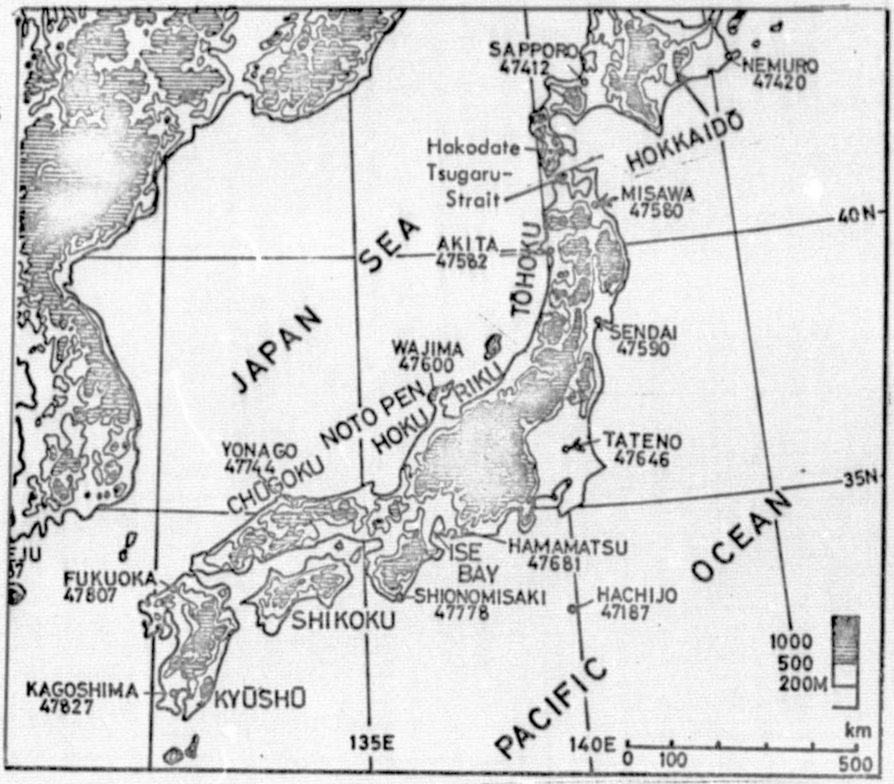

Fig. 1 Aerological Stations and international station number.

Names of districts are also indicated.

Fig. 2

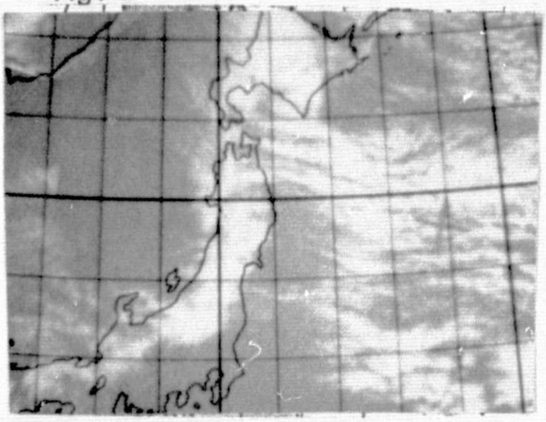

Fig. 3

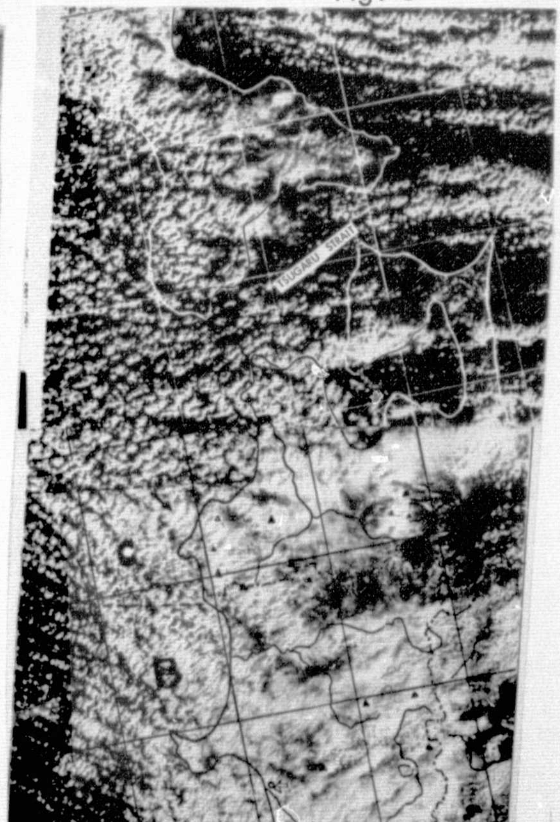

Fig. 2 ESSA-8 APT picture.
01 GMT 15 Dec. 1972.

Fig. 3 LANDSAT picture showing the detailed structure of the clouds.
01 GMT 15 Dec 1972.

by meteorological satellite pictures and clarified the relationship between the vertical wind shear and three types of cloud orientation longitudinal, transversal and cellular and also some meso-scale features of clouds. Neither meteorological nor aerial photographs have been able to show mesoscale feature of clouds in its entirety due to poor resolution in case of the former and to the limitation of the coverage of the area in case of the latter.

An example of an extensive view of cloud distribution over and around Japan associated with an extremely strong cold air outbreak with strong wind is shown in Fig. 4 which was taken by a meteorological satellite EESA. The picture shows large orographical effects on cloud distribution. It also indicates well defined cloud streets of several hundred kms length, however it is hard to obtain an information on cloud type and structure from this picture. Mesoscale features of the clouds as observed by LANDSAT and meteorological condition will be described in the following section.

3.1 Clouds under a moderate winter monsoon

Clouds under a weak cold air outbreak with moderate wind speed in northern Japan is already shown in Fig. 3. Since half a degree of latitude is equal to 55 kms in length, the size of clouds can be easily known. The surface weather map and radio sounding at Akita (location is indicated by an arrow in Fig. 3, also see Fig. 1) at 00 GMT are shown in Fig. 5 (A) and (B).

The surface weather map shows that a sharp pressure gradient is limited to northern Japan with a migrating high in the central part of the Japan Sea. The cloud type observed at the surface ie eigher towering cumulus or cumulo-nimbus. Although it is not shown in the figure, snow in the neighborhood is observed at Akita. Comparing Fig. 3 with Fig. 5 (A) it is found that cumulo-nimbus has a fuzzy appearance in the LANDSAT picture and beneath the cloud snow is falling.

The distribution of relative humidity in Fig. 5 (B) indicates humid layer between 1.5 and 3 kms suggesting existence of cloud in the layer. The wind speed is fairly strong in the northern Japan as are shown in the upper air charts of Fig.6. The fact unusually little cloud coverage over the Japan Sea is due to the fact that a migrating high exists in the central part of the sea.

The general direction of cloud orientation is nearly parallel to the average wind at 850- and 700-mb levels or cloud layer. Some features of clouds are described below.

In the area indicated by a letter A the convective cloud elements line up in rows. This row of cloud elements in the direction of wind is defined as "Cloud Street". The average distance of eleven cloud streets is found to be 5.54 kms. If the height of the small cumuli is assumed to be 1 km, the height to width ratio is 1: 5.54 which is same order of magnitude to that found for the tropical region by Kuettner (1971) while the

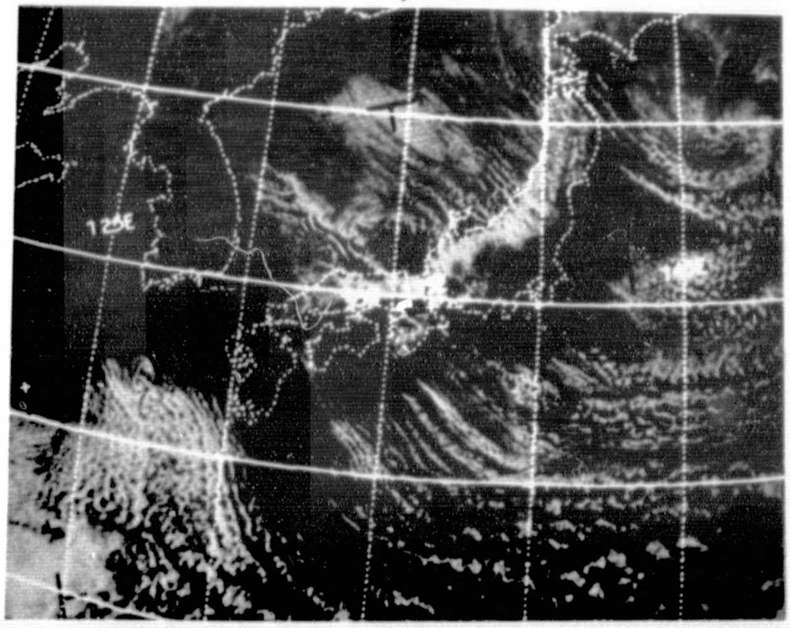

Fig. 4 Cloud distribution associated extremely strong cold air outbreak as seen by meteorological satellite ESSA.

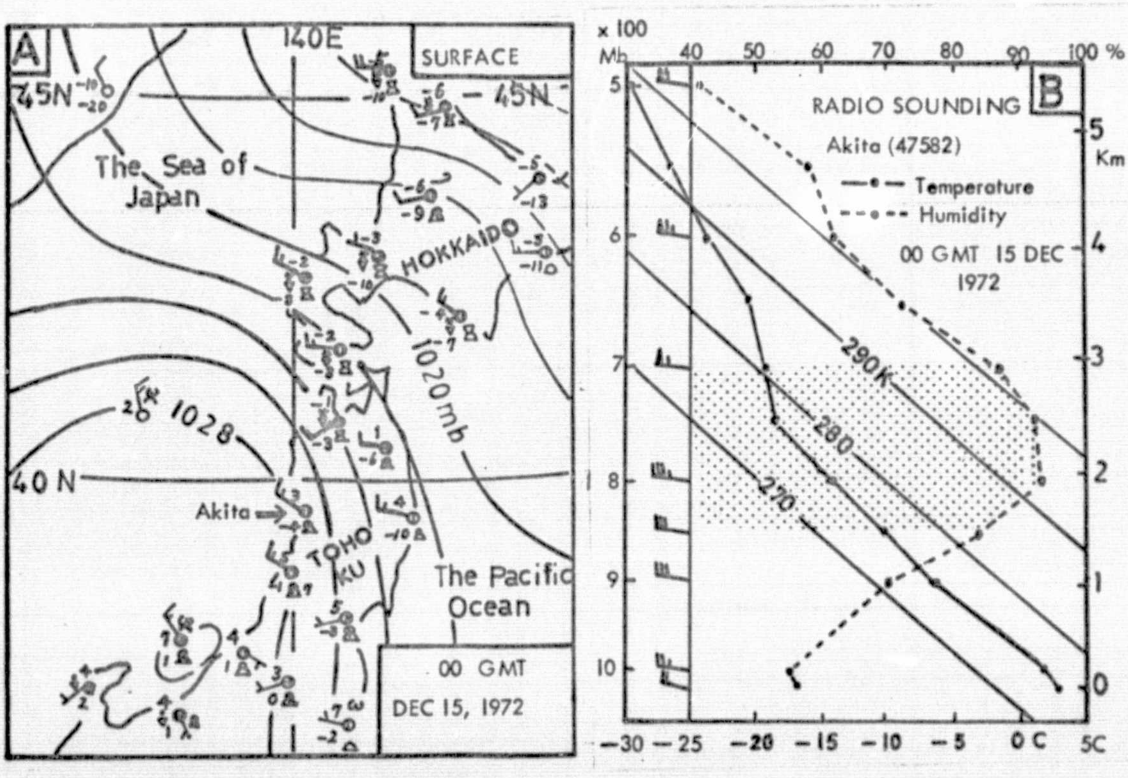

Fig. 5 Surface weather map (A) and radio sounding at Akita (B).
00 GMT 15 Dec 1972.

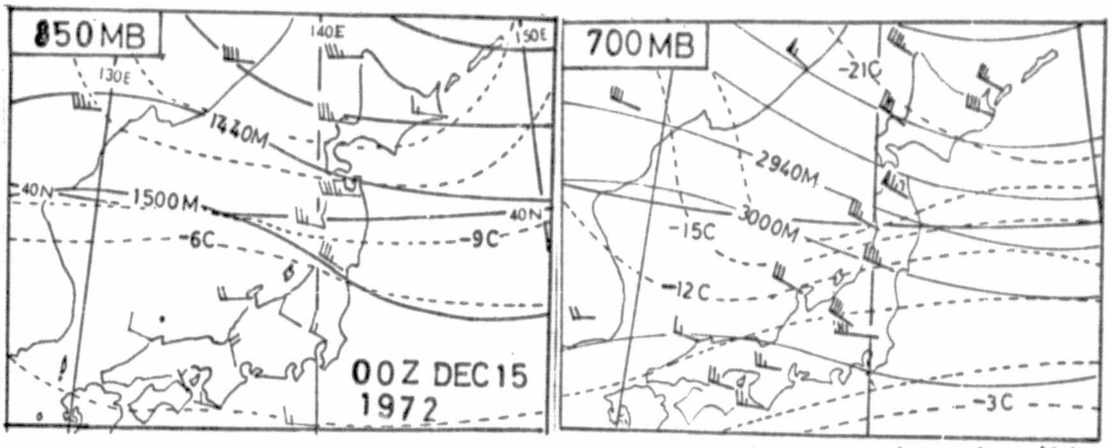

Fig. 6 850- and 700-mb charts. Contours and isotherms are shown in solid and broken lines. 00GMT 15 Dec 1972.

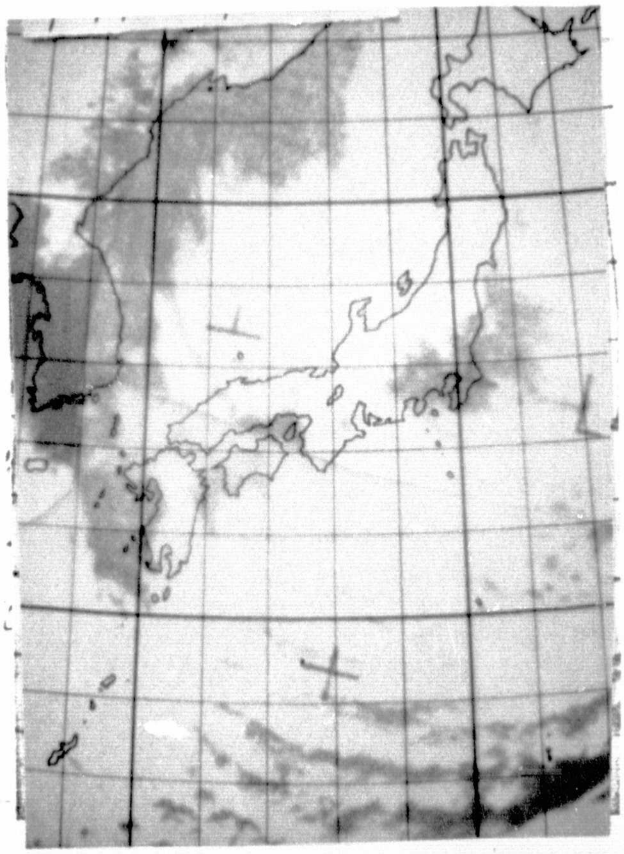

Fig. 7 ESSA-8 APT picture showing cloud distribution associated with strong cold air outbreak. 01 GMT 2 Dec 1972.

average spacing of individual cloud elements along the street is 2.4 kms. In the area indicated with a letter B, both the width of cloud streets and distance of cloud streets become wider and the average distance of the streets is 10 kms.

Mi... ..c analysis indicates the cloud streets are composed of very narrow banded clouds aligned perpendicularly to the cloud streets. Here these small clouds are defined as "Transversal Cloud". The spacing of these small narrow transversal clouds defined as "Wave length" for short ranges from 1.6 to 2.1 kms. The cloud street indicated with an an arrow in the area C shows transversal cloud with wave length of 4.2 kms in average. It seems that these larger transversal clouds are partly effects of a small mountain range in the coast. In the picture, mountains higher than 1 km are indicated in dark solid triangles while near the coast mountain higher than 600 meters is shown in an open triangle.

There is a slight positive correlation among width of cloud streets, wave length of transversal clouds and width of indicidual clouds. The ratio: width of cloud street to wave length of narrow transversal clouds of well defined ones are in average 4 in the area B while it is 3 in the area C where both width of the streets and individual transversal clouds are larger than those of the area B.

As to the relationship between vertical wind shear and cloud orientation, if an assumption is made that the cloud exists where relative humidity is larger than 85 % the cloud top at Akita will be 3 kms while the height of small cumuli off the coast is estimated to be 1 km or less. Then the average vertical wind shear between the the surface and the cloud top at Akita is 0.008 /sec and it will be larger for small cumuli seen off the coast. The criterion proposed by present author (1967, 1974) for longitudinal cloud was larger than 0.007/sec therefore the criterion is well satisfied, and the criterion obtained through meteorological satellite is also applicable in this case provided that clouds aligned in the direction of the wind direction as are seen in Fig. 3 are all longitudinal clouds.

3.2 Clouds under strong cold air outbreak with long trajectory over the sea

The clouds under strong clod air outbreak taken by Meteorological satellite ESSA-8 is shown in Fig. 7 while those taken by LANDSAT is shown in Fig. 8 which covers a strip of 180 kms width in the western part of the area shown in Fig. 7.

In order to see the degree of monsoon the variation of temperature and winds over Kagoshima (47827) and Naze (47909, 28.4 N, 129.5 E, 295 m) at 500- and 900-mb levels are plotted and shown in Fig. 9 for the period of 00 GMT Dec. 1 and Dec. 4 at 12 hours interval. In the figure the average temperature of December 1972 is shown in solid lines. From the figure it is easily known that the temperature at picture taking time was much colder than the average especially at 500-mb level or at the height of 5.7 kms. At Kagoshima the wind speed at 500-mb level at 00 GMT of Dec. 1 was the strongest of the month and was still very strong at the picture time.

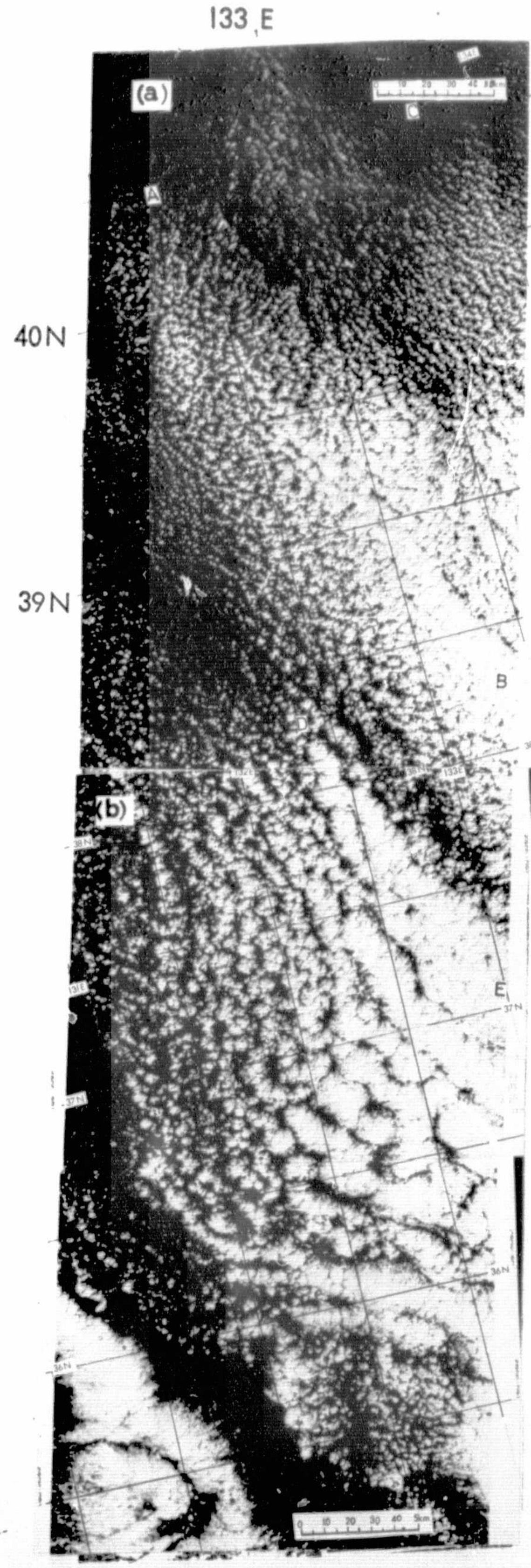

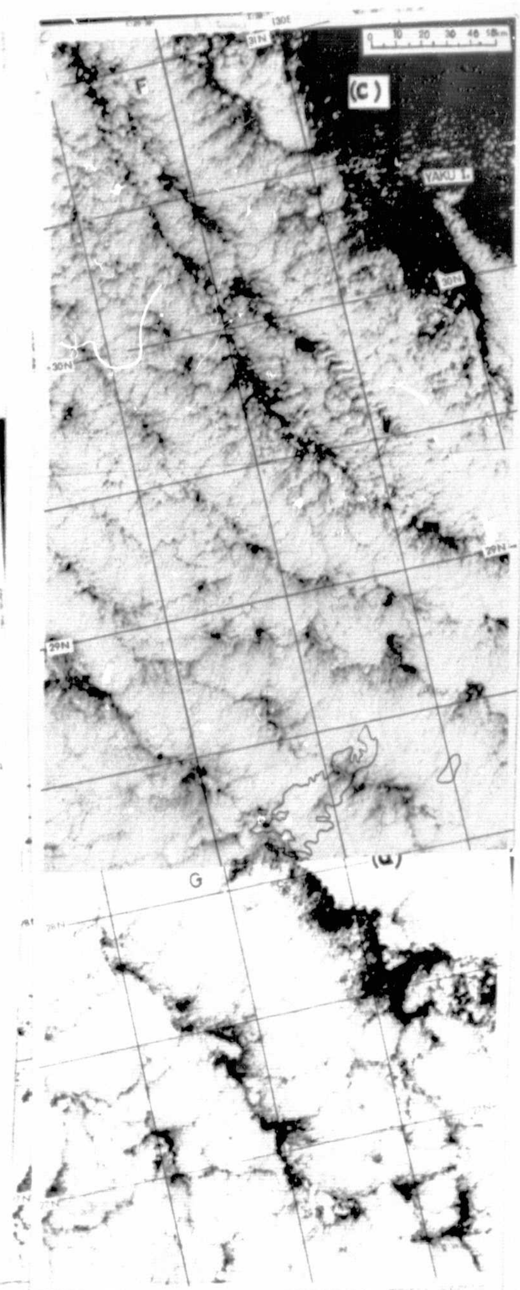

Fig. 8 LANDSAT pictures showing detailed structure of the clouds. 01 GMT 2 Dec 1972.
Left: Over the Japan Sea
Right: Over the Pacific Ocean

The surface weather map at 00 GMT Dec. 2 1972 approximately I hour before satellite pass is shown in Fig. 10 which shows a typical pressure pattern in winter around Japan. The clouds observed at the surface are predominantly convective type and at Naze located in the island shown in Fig. 8 towering cumulus with shower is observed.

As to the structure of clouds, it is seen from Fig. 8 that the clouds which have an appearance of continuously stratified clouds in ESSA–8 APT picture shown in Fig. 7 consist of many convective cloud elements. Some of the features obtained from Fig. 8 are described below.

The average distance of cloud streets found in the area marked with a letter C is 3.43 kms. Following the clouds from a point A south-eastwards to point B, one can see that scattered cumuli develop and organize themselves into a large cloud street. For instance small scattered cumuli develop into a solid cloud street of 18 kms width at B located 270 kms downstream from A. In the south the development takes place in shorter distance as is seen in the cloud street between D and E. At the point E which is 150 kms downstream of D, the width of the solid cloud street is as wide as 45 kms. With increasing cloud width, the distance of cloud streets also increases and the average width of the streets south of D is 15 kms.

Comparatively well defined wide cloud streets are seen in Fig. 8 (C) furhter south of the area in the previous figure and located in the Pacific Ocean over the warm ocean current Kuroshio. There is a tendency that the distance of cloud streets becomes wider towares down stream. In the northern part of figure (c) the average distance of cloud streets is 25.5 kms ranging rom 20 to 28 kms while it increases to 33.8 kms with the range of 30 to 40 kms in the downstream.

The fairly well defined transversal wave clouds are seen in the area marked with a letter F with an average wave length of 8.6 kms and cloud street width of 46 kms. The ratio, cloud street width to wave length is 5.35. Further larger transversal wave clouds are seen in the area marked with G. Here wave length of four wave clouds in average is 16.5 kms and the cloud street in average is as wide as 70.2 kms thus the ratio, cloud street width to wave length is 4.25.

The radio sounding at Naze located in the island shown in Fig. 8 is plotted and is shown in Fig. II. The relative humidity distribution indicates that the cloud may exist between I.2 and 2.I kms. Here the average vertical wind shear is 0.0052/sec which is according to the criterion proposed by the present author is transversal clouds or mixed type of longitudinal, transversal and cellular type may coexist. Thus the criterion obtained from meteorological satellites is applicable to this case, too. It is also found that this type of cloud does not cause rainfall of moderate intensity. If it rains it is weak shower.

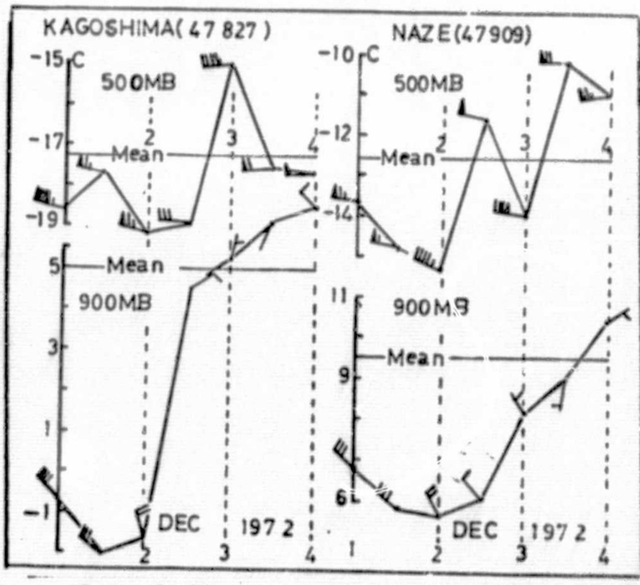

Fog. 9 The variation of temperature and winds at 900- and 500-mb levels at Kagoshima and Naze.

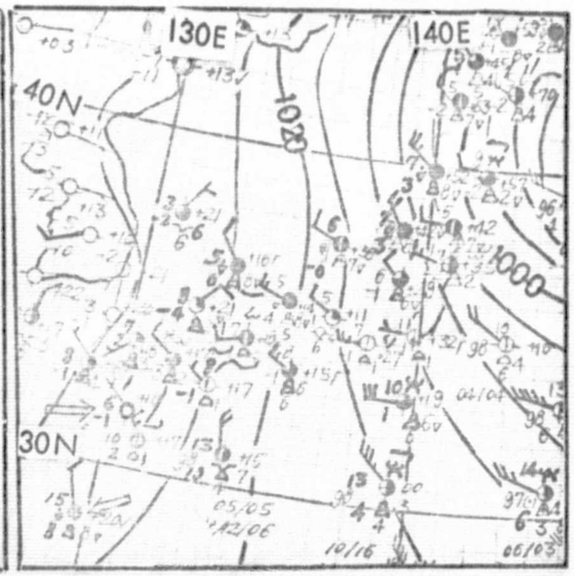

Fig. 10 Surface weather map at 00 GMT Dec 2 1972. Upper and lower arrows indicate Kagoshima and Naze respectively.

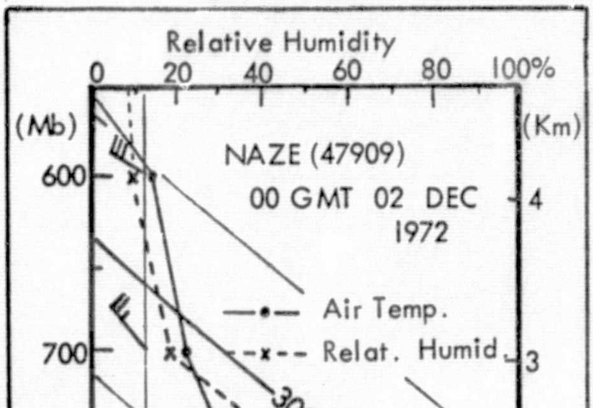

Fig. 11 Vertical distribution of temperature, winds and relative humidity plotted on an Emagram. Naze, 00 GMT Dec 2 1972. Diagonal solid lines are dry adiabats or equipotential temperature lines.

4. MOUNTAIN LEE WAVE CLOUDS

Parallel rows of clouds in the lee of a mountain range are popularly known as mountain lee wave clouds (hereafter it is abbreviated as MLWC for short). Formation of MLWC takes place any time if a meteorological condition for its formation is satisfied. According to the experiences of present author in the analysis of meteoro logical satellite pictures, however, the appearance of MLWC in APT pictures in and around Japan is limited to the period of cold season. The main reason for the limitation of the period is considered due to the fact that strong persistent wind in the lower troposphere is limited to cold season around Japan. Thus MLWC is considered one of the particular phenomena of winter monsoon clouds.

Doos (1962) and Fritz (1965) made studies of MLWC based on meteorological satellite TIROS pictures. Both of them satellite pictures simply to get wave length without going into detailed analysis. Taking advantage of high resolution of LANDSAT picture a detailed nalysis of MLWC is attempted.

4.1 The feature of mountain lee wave clouds

In Fig. 12 is shown the example of MLWC as observed by LANDSAT. In the pcitures latitudinal and longitudinal lines are drawn every half a degree. Since half a degree of latitude is equal to 55 kms the size of clouds and wave length can be easily known from the picture. It should be also mentioned that there are so many examples of MLWC in LANDSAT pictures.

Careful inspection of figure (a) indicates that MLWC of 4 different wave length, two MLWC to the north of the main MLWC and one to the south of MLWC. A similar feature is seen in figure (b), too.

A microscopic analysis indicates that individual cloud is consisted of one order of magnitude smaller elements. This feature is most clear in the clouds of figure (b), for instance the long and wide cloud in the central part of the picture reveal that the cloud is consisted of many narrow clouds arranged perpendicularly to the main cloud. The average spacing or wave length of these small transversal clouds is 1.8 kms. The clouds in figure (a) also indicate a similar feature although less distinctive. Some parameters of MLWC are summarized and shown in Table I.

It should be mentioned that there are many other examples besides those shown in Fig. 12, and in general MLWC over the sea is more distinctive with well defined wave length than those over the land of complicated topography where degeneration of MLWC takes place due to interference of waves and also due to orographical effects.

(a) Dec 1 1972

(b) Jan 4 1973

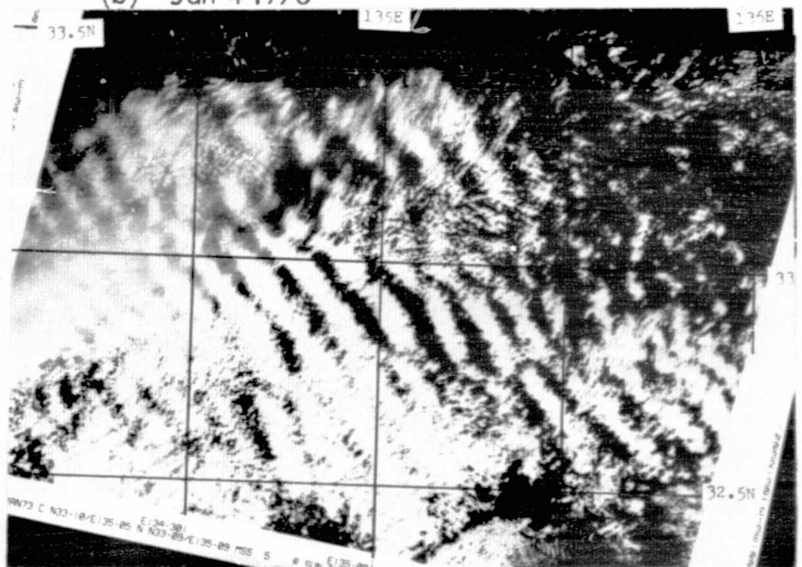

(c) Feb 6 1973

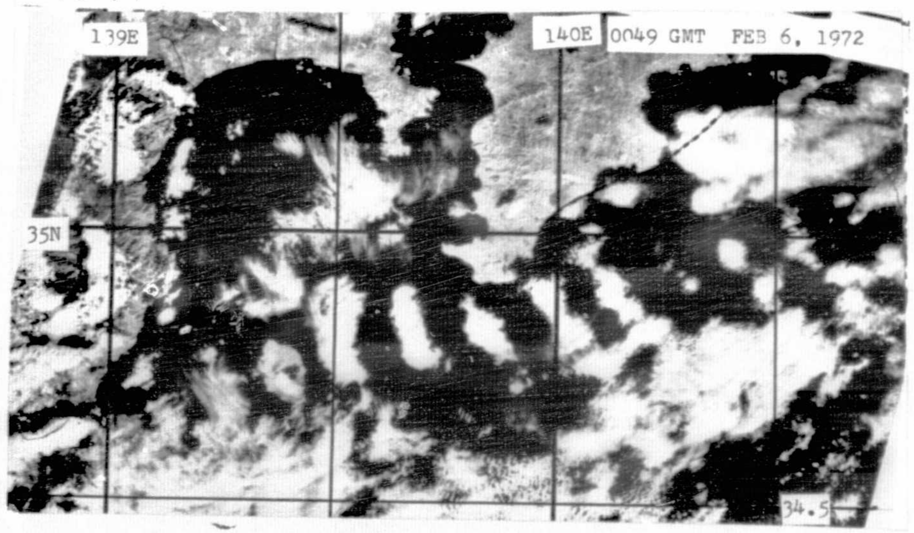

Fig 12 Examples of mountain lee wave clouds in LANDSAT pictures. The time of observation is approximately 00 GMT.

Table 4.1 Some parameters of mountain lee wave clouds obtained from LANDSAT pictures

Date	Number of cloud	Wave length (km) Mn (km)	Mx (km)	Av (km)	Mx width of cloud (km)	Mx length of cloud (km)
Dec 1 '72	(1)* 5	15	22	17.8	6	12
	(2) 3	18	20	19.0	10	26
	(3) 6	12	18	14.5	8	16
	(4) 6	15	18	16.2	8	42
Jan 4 '73	(1) 13	8	12	9.2	9	39
	(2) 13	6	11	8.8	9	49
	(3) 14	7	13	10.8	9	9
Feb 6 '73	8	11	15	13.1	8	90

Note. : The order of numbering is from north to south.

4.2 Meteorological feature

Taking the example of Dec 1 case, a detailed analyses on synotic meteorological situation is made. The surface weather map covering Kyushu and its surrounding is shown in Fig.13. The type of clouds observed at the surface is predominantly cumulus. As was mentioned in the previous section the wind speed on this day is very strong. The vertical structure of the atmosphere over Kagoshima located in the upstream of the MLWC is shown in Fig. 14 in which airtemperature, wind speed and direction as well as the average wind speed of the month are shown. On the right hand side is shown the vertical distribution of relative humidity.

The relative humidity distribution indicates humid layer between 1.5 and 2.0 kms suggesting the existence of the cloud in this layer. The wind speed at 1.5 and 2.0 kms or cloud top level is 20 and 30 m/s respectively.

Temperature distribution indicates a sharp inversion at 2.5 km level. Wind speed distribution is fairly complex with a few maxima and minima. It is interesting to notice that in the lcoud layer or high relative humidity layer both wind speed and direction are nearly uniform. Wind speed as a whole is stronger than the average.

Upper air charts from 1000- to 300- mb levels are shown in Fig.15. Air temperature and relative humidity are plotted in the unit of Centigrade and percentage. Contours are drawn every 30 meters below 800-mb level, every 50 meters at 700- and 600-mb

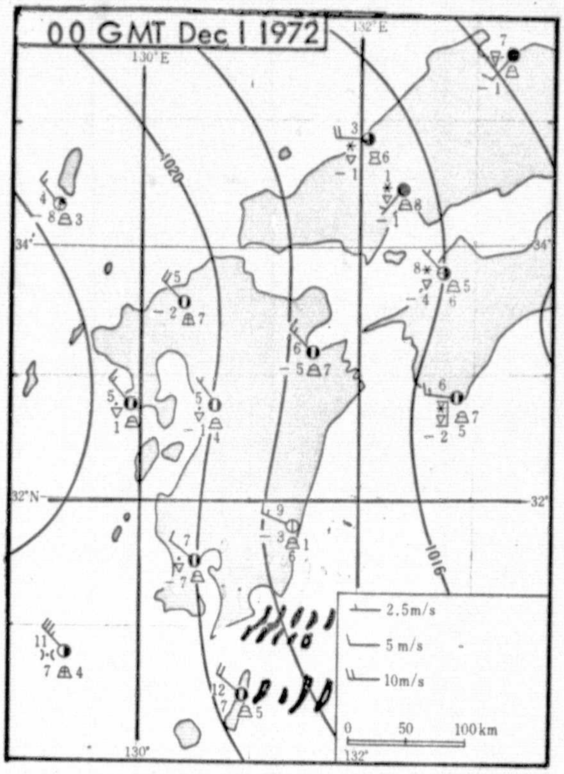

Fig. 13 Surface weather map of western Japan. 00 GMT Dec 1 1972. Isobars are drawn every 2 mbs.

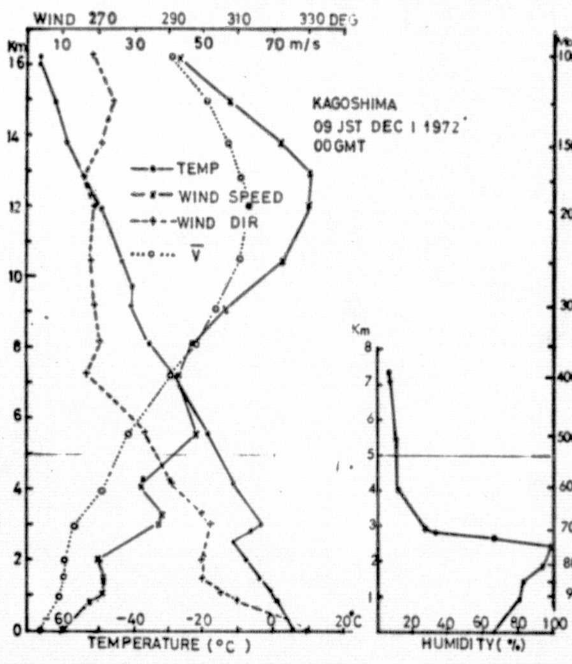

Fig. 14 Vertical structure of atmosphere above Kagoshima. 00 GMT Dec 1 1972. Air temperature, Wind speed and direction, average wind speed of December 1972 and relative humidity are indicated. V is the average wind speed of Dec 1972.

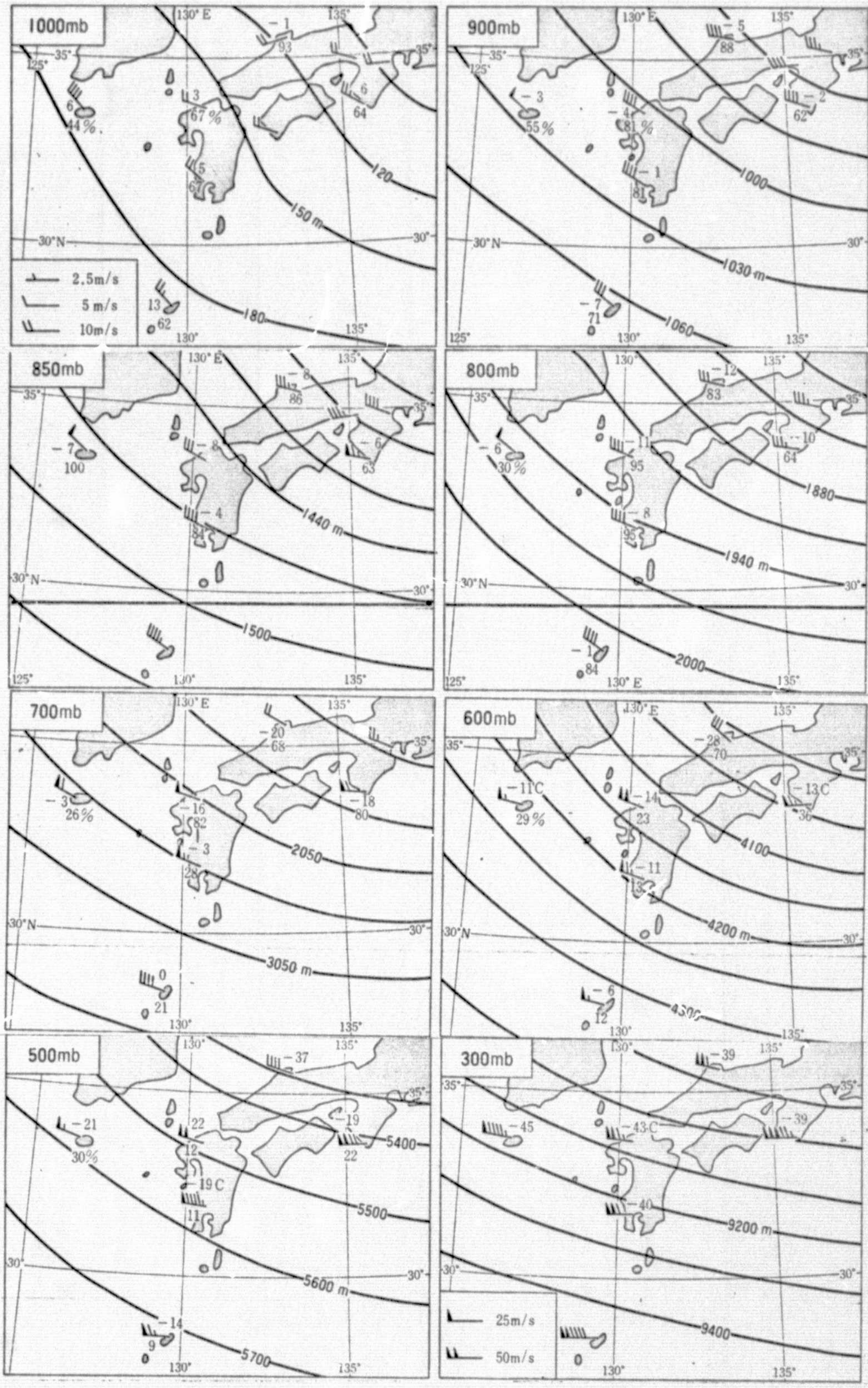

Fig. 15 Upper air charts at 00 GMT Dec 1 1972. Solid lines are contours in geopotential meters. Air temperatures and relative humidity are are also indicated in Centigrade and %.

levels and every 100 meters at 500- and 300-mb levels. It is seen that the direction of the contours are fairly consistent throughout the layer and wind is also strong where MLWC exists.

Vertical structure of the atmosphere on Feb 6 1973 at Tateno and Hamamatsu are shown in Fig. 16. Hamamatsu is located about 148 kms upstream of the island seen in Fig. 12 (c) where MLWC begins to appear while Tateno is 160 kms NNE of the island.

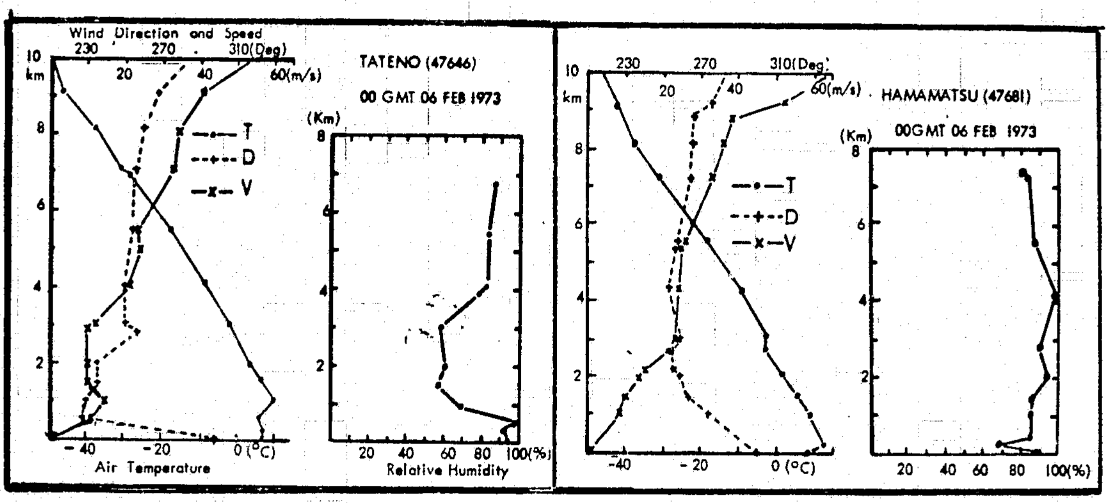

Fig. 16 Vertical structure of the atomosphere observed at Hamamatsu and Tateno at 00 GMT Feb 6 1973. In the figure T, D and V represent air temperature, wind direction and wind speed respectively. Relative humidity is also shown in the right hand side in %.

The vertical structure of the atmosphere above Hamamatsu and Tateno is different from that of the previous case. In this case the relative humidity is high above 4 kms, which is rare case at this season. The wind speed is fairly strong, however not so complicated as before. The height of the clouds of MLWC in Fig. 12 (c) estimated from the shadow is 3 kms and wind speed at cloud top level is 3 kms. The wind speed at the height of 1.5 kms and cloud top level when MLWC is recognized are shown in Table 2 for 4 examples.

Table 2 Wind speed at 1.5 kms level and cloud top levels when MLWC appears in LANDSAT pictures. Unit: m/s

Date / Height	Dec 1 '72	Jan 4 "73	Feb 6 '73	Mar 4 '73
1.5 kms	20	12	10	13
Cloud top	28	23	23	19

The analysis of wind structure indicates that wind speed at 1.5 kms is stronger than 10 m/s and at the cloud top level it is more than 19 m/s.

4.3 Wave length

Döös (1962), Foldvik (1962) derived the equation to estimate wave length (λ) of a mountain lee wave under the assumtion that Scorer parameter has exponential distribution. In the present case the computation of Scorer parameter based on the actual wind and temperature distribution indicates far from exponential distribution. In their application to the actually observed ones they also made very large smoothing in temperature and wind distribution. Here instead of doing smoothing in Scorer parameter an attempt is made to apply the most simple equation, one layer model or parcel method expressed in Eq. (1).

$$\lambda = 2\pi \overline{U} / \sqrt{g \frac{d}{dz} \ln \theta} \tag{1}$$

where U, θ and z denote representative wind speed, potential temperature and vertical coordinate respectively. The result of the computation is shown in Table 3.

Table 3 Wave length computed using one layer model

Date	H	$\overline{U}$ (m/s)	Wave length (km)	
			Observed	Computed
Dec 1 '72	9.2	39	16.8	17.8
Jan 4 '73	9.1	27	9.6	13.2
Feb 6 '73	8.0	29	13.1	12.9
Mar 4 '73*	10.2	25	14.7	12.5

Note. *: The picture of this case is not shown in this report.

The result indicates a good correspond. in spite of the fact a large assumption is involved. A similar result is also obtained by Fritz (1965). A large discrepancy of Jan. 4 case is partly due to the fact that the data used for computation is that of the station located far from the area of MLWC.

5. MESO-HIGH

A small anticyclone which is one order of magnitude smaller than an ordinary anticyclone is called a meso-high. This kind of anticyclone is difficult to detect in a routine synoptic weather map analysis due to its small size. Formation of a meso-high frequently takes place associated with a well developed thunderstorm. It is also formed due to an orographical effect although the one formed due to this effect is less distinctive. A well developed meso-high affects not only local wind but also cloud distribution (Fujita, 1962).

During the study of winter monsoon cloud distribution in Hokkaido based on LANDSAT picture, a narrow area of less cloud coverage is recognized as is indicated in Fig. 17. It is generally considered that this is due to the influence of Mt. Shakotan (height: 1255 meters) located in the upstream.

A question arises in the following two points, i. e. i) if this cloud distribution is simply due to an orographical effect alone or not, ii) what type of pressure pattern exists from mesometeorological point of view.

5.1 Mesometeorological analysis

The regular synoptic weather map is already shown in Fig. 5 (A) in which very weak pressure ridge is analyzed over Hokkaido. In the upper air charts of 850- and 700-mb levels shown in Fig. 6 no particular pressure ridge is recognized which is natural since no aerological stations exist in the inland area.

Based on all available data gathered later a mesometeorological analysis is made to find out actual pressure pattern over Hokkaido and is shown in Fig. 18. In the figure a meso pressure ridge is indicated in broken line. The effect of which is clearly recognized in the wind direction inside the meso-ridge area. It is sure that topographical influence on the wind direction is large, however it seems that this meso ridge has an influence on the wind direction, too.

Since there is no radio sounding stations in the inland area, vertical extent of the meso-ridge is hard to estimate. As to the influence on the cloud distribution although it is not known quantitatively it is considered that there is a certain influence even if it may not be so large as orographical effect.

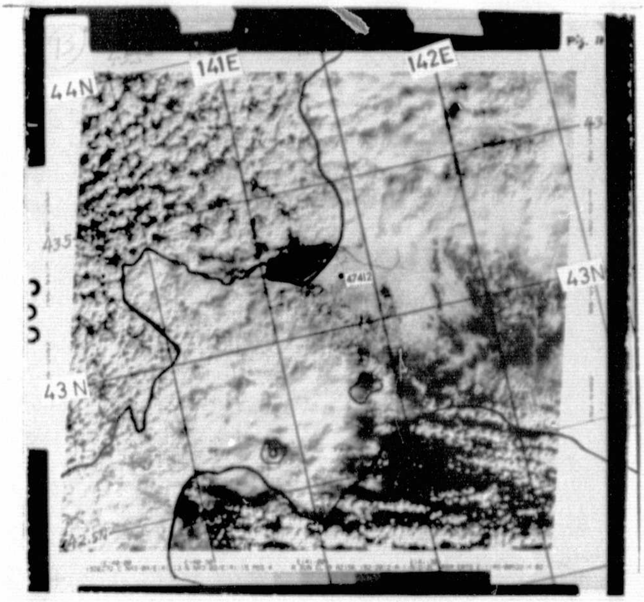

Fig 17 LANDSAT picture showing cloud distribution over Hokkaido. 01 GMT Dec. 15 1972.

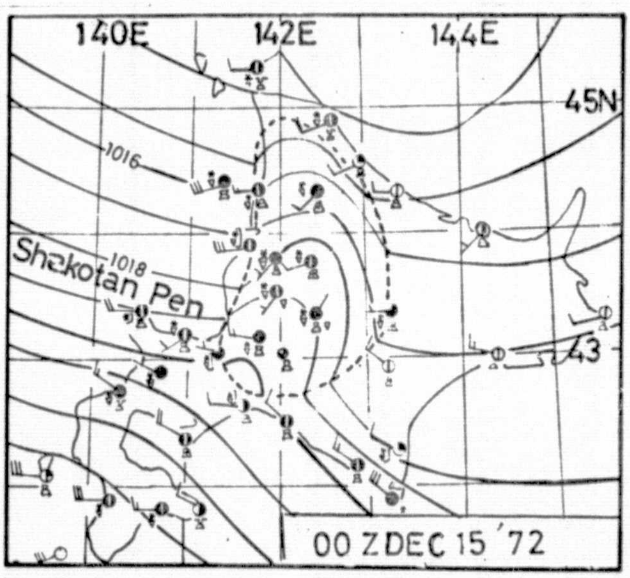

Fig. 18 A mesometeorologically analyzed weather map. A high pressure area is surrounded with a broken line. 00 GMT Dec 15 1972.

6. SNOW COVER

Both snowfall and snow cover are influenced by orographical features thus it is difficult to get an exact snow cover chart. In order to fill up the lack of observing station networks Ishihara (1967) developed a method of estimating snow depth taking topographical parameters into account. In Japan Meteorological Agency (hereafter it is abbreviated as JMA), snowfall and snow cover charts are made operationally during cold season.

Since the networks of daily reporting weather stations are not enough, the observations at railway and hydroelectric power stations are also used. The reports from these stations are of great help yet far from satisfactory to draw snow cover chart accurately.

Although there are several studies to fill up the lack of observation networks, no special methods are applied in drawing isolines in operational meteorological services. Thus snow cover charts are made subjectively by individual persons based only on the reported data. A LANDSAT picture can show at least snow cover area correctly even if it may not show depth explicitly. An attempt is made to study feasibility of applying a LANDSAT picture for drawing isolines in a snowcover chart.

6.1 Comparison of snowcover chart drawn operationally and that made in reference with LANDSAT picture and other sources

Fig. 19 (a) is a carbon copy of snow cover chart made at JMA operationally based on the daily reported data. In the figure iso-lines are drawn more than 10 cm snow depth. Comparing this figure with a LANDSAT picture shown in figure (b) it can be recognized that the figure shown in figure (a) is not accurate even if the LANDSAT picture does not show depth. Figure (c) is the snowcover chart drawn based on all the available data gathered later and the LANDSAT picture. It can be easily known that the chart thus made is different from figure (a) especially in the mountainous area (as to topography see Fig. 1). It should be mentioned that even if figure (c) is greatly improved the actual distribution in the mountainous area will be a little different since the data are not enough.

Following same procedures a snow cover chart of south-western Hokkaido is made and shown in Fig. 20 (a), (b) and (c) respectively. It is found that a flat area looks more bright than mountainous areas if the snow depth is equal.

A great effort is made to estimate snow depth based on a LANDSAT picture however it is extremely difficult to get proper value.

Since snowcover is persistent during cold season LANDSAT pictures, even in 18 days interval are found to be of great help in drawing snowcover chart.

(a) Unit: cm

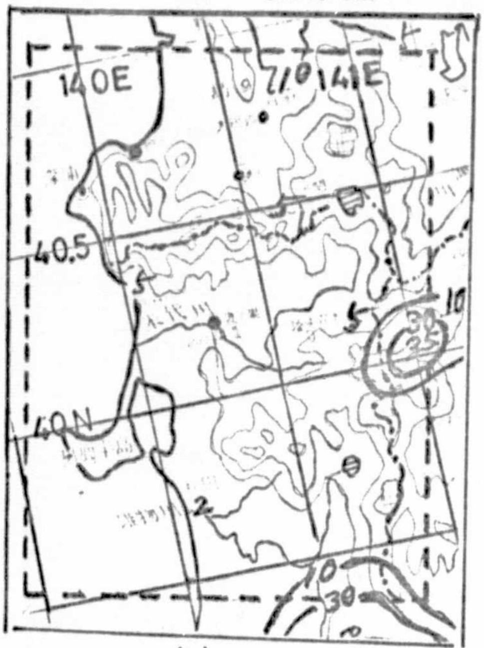

(b)

(c)

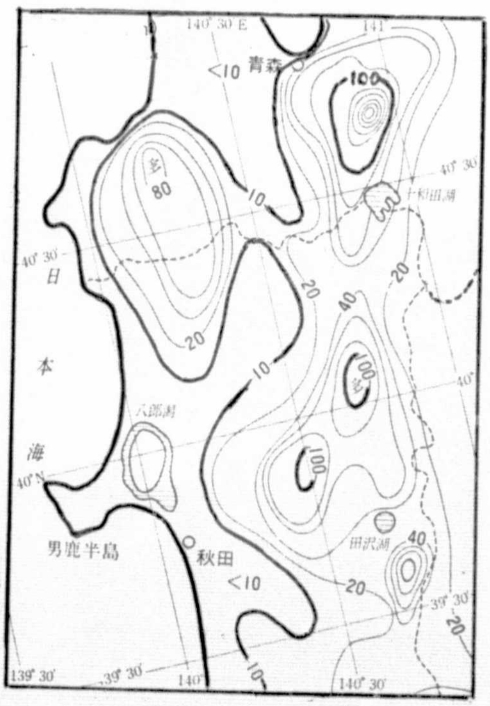

Fig. 19 Snowcover charts and LANDSAT picture. (a) is a carbon copy of snow cover chart operationally made at JMA. (c) is made in reference with LANDSAT picture and all other available data. (b) is a color composite of LANDSAT MSS data.
In figure (a) numerals are the snow depth observed at weather and railway stations and thin solid lines are contours of 200, 500 and 1000 meters above MSL. The thick broken line is the boundary of LANDSAT picture.

(a)

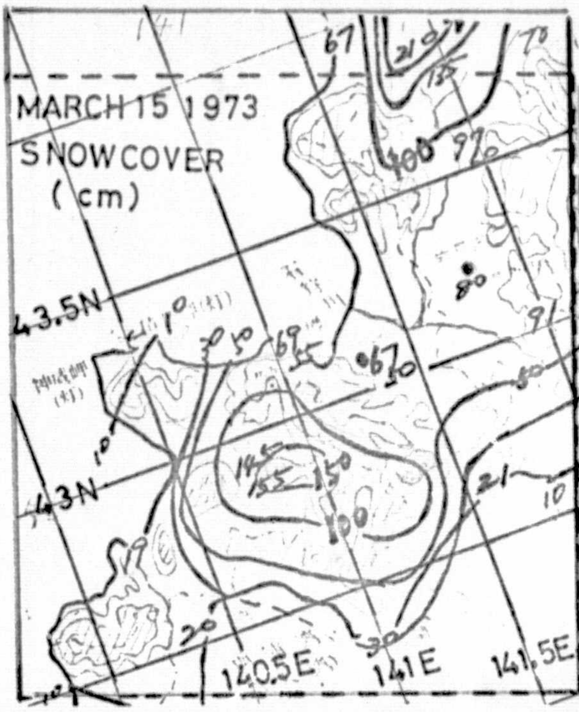

(b)

(c)

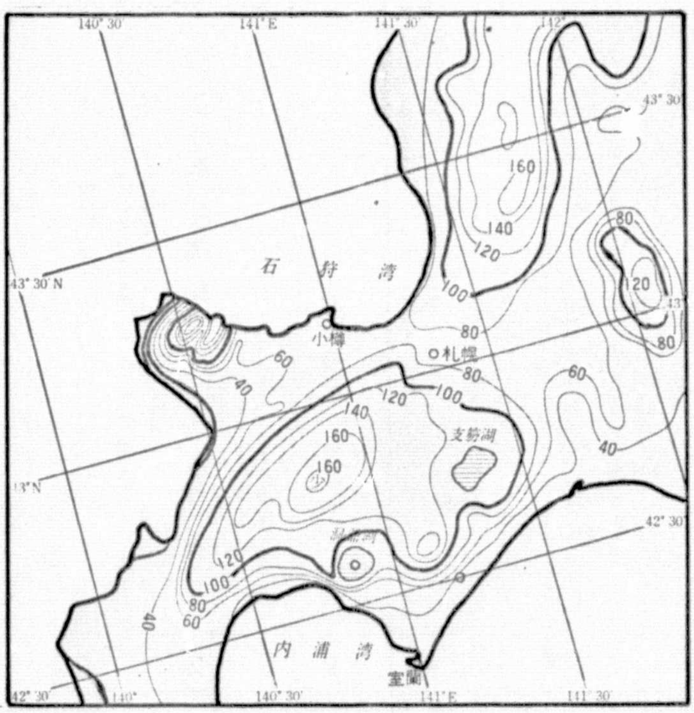

Fig. 20 Snowcover charts and LANDSAT picture. (a) is a carbon copy of operationally made snow cover chart at JMA, (c) is the snow cover chart made based on LANDSAT picture and all other available data.

7. CLEAR AIR TURBULENCE

All turbulence in the free atmosphere of interest in aerospace operations that is not or adjacent to visible convective activity is fefined as CAT (Clear Air Turbulence). This cinludes turbulence in cirrus clouds not in, or adjacent to visible convective activity.

Both static and dynamic stability contribute to its formation. Large wind shear is found in the vicinity of a jet stream therefore the vicinity of a jet stream has a high potential for CAT. Since it is difficult to pin point an area of high potential for CAT it is one of the greatest problems in the field of aeronautical meteorology.

Viezee (1966) based on the analysis of TIROS pictures pointed out that CAT occurs in the vicinity of a jet stream where cirrus exists. On Aug. 29 1972 LANDSAT made an observation of the area of CAT in northern Japan. Some meteorological features will be described below.

7.1 CAT of Aug. 29 1972 and the features of clouds

The pilot reports on the CAT is plotted on the flight cross section chart and is shown in Fig. 21. It indicates that T33 and B227 encountered moderate CAT above the Tsugaru strait between 00:20 and 00:40 GMT respectively, and the height was at 25,000 and 26,000 fts.

The picture taken from LANDSAT is shown in Fig. 22. Since the time of observation was 00:52 GMT it can be considered almost simultaneous to CAT occurrence. The picture shows interesting clouds. The clouds in the area indicated with a letter "d" with a shape of a tadpole suggest strong wind and wind shear in vertical direction. The upper air chart shown in Fig. 24 indicates the clouds are actually in the jest stream area.

The clouds in the areas indicated with letters "a", "b" and "c" have an outlook of cirrus. The clouds in the area "a" aligned meridionally indicate a turbulence with wave length of 14 to 20 kms, while the clouds in the areas "b" and "c" suggest cirrus extended from convective activity. In order to see the relationship with meteorological situation meteorological analyses are made.

7.2 Meteorological analysis

The surface weather map and upper air chart of 300-mb level are shown in Fig. 24 respectively. The weather stations in the vicinity of CAT indicate the observation of cirrus. In the area to the north of CAT area fair weather cumulus is observed while in the area to the south of CAT area middle and low level clouds are observed.

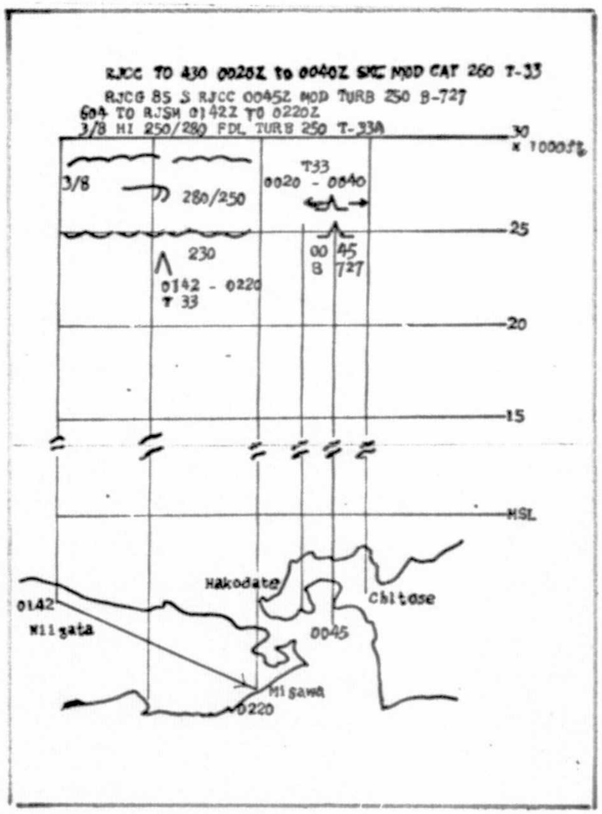

Fig. 21 The flight cross section made based on pilots' reports.

Fig. 22 LANDSAT MSS picture showing the clouds in the vicinity of CAT. 00:52 Aug. 29, 1972.

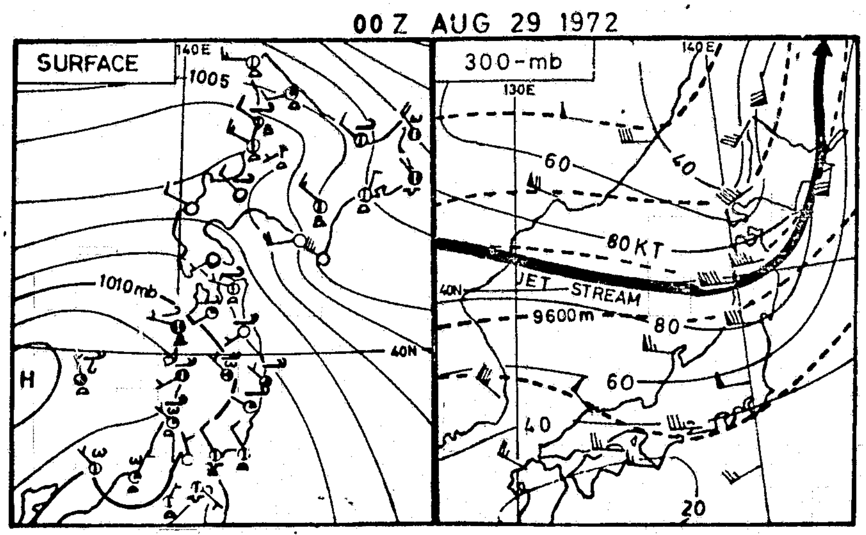

Fig. 23 Surface weather map and 300-mb chart. 00 GMT Aug 29 1972. In 300-mb chart a thick solid line represents a jet stream axis.

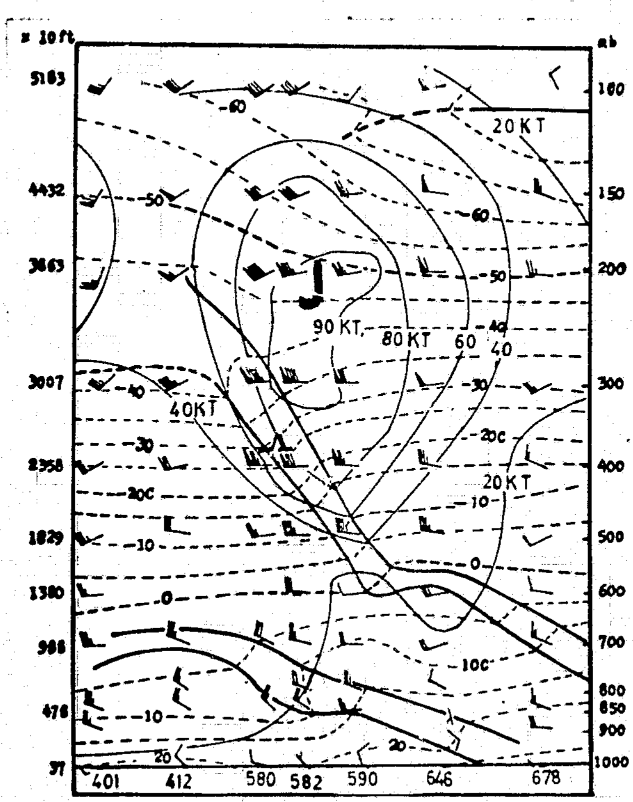

Fig. 24 The cross section chart along 140°E meridian. Isotherms and isotachs are shown in broken and thin solid lines and thick solid line represents the bountary of inversion layer. 00 GMT Aug 29 1972.

The 300-mb chart shows the jet stream curves sharply cyclonically in the northern Japan. It is seen that the clouds in LANDSAT picture are on the left hand side or cold air side of the jet stream axis.

The vertical structure of the atmosphere along 140°E is shown in Fig. 24 in which isotherms, isotachs and actual wind observations are shown in broken and thin solid lines and international symbols. The units used are centigrade and knot respectively. Thich solid lines represent the boundary of inversion layer, and letter J denotes jet stream.

It is found that the level of CAT is at the base of the inversion layer where the vertical wind shear is the maximum. The value computed is 0.0167/sec.

8. THIN CIRRUS AND RADIATION CHARACTERISTICS

Thin cirrus is often very difficult to detect in a meteorological satellite picture. In the interpretation of satellite data especially infrared radiation data, it is important to detect thin cirrus. A feasibility study is made on the possibility of recognizing it based on MSS data. The study on radiation characteristics of ground surface and cirrus are also made.

8.1 Pictorial representation of LANDSAT data

Fig. 25 is the pictorial representation of LANDSAT MSS Band 4 and 7 data respectively. Comparing two pictures spectacular difference is easily een borth over the land and the sea, i. e. the cloud clearly visible in Band 4 picture d isappear in the picture of Band 7 which suggests a certain type of cloud can be distinguished if the different spectrum of MSS data are available.

In reference with the surface observation the white fan shaped ones are cirrus. Characteristics of this cirrus in connection with meteorological situation will be discussed in the following section.

8.2 Meteorological situation

Surface weather map is shown in Fig. 26 which indicates that partly cloudy thin cirrus extensively over the land. At Nagoya, the largest city in the central Japan with poputlation of a little over 2 millions smog is also observed. The numerical values of visibility in the area of the picture are also plotted in the unit of km.

At two radio sounding stations in the area, Hamamatsu (47681) and Shionomisaki (47778), thin cirrus is observed although it is difficult to recognize it in the picture. The result of the observations is plotted on an Emagram and shown in Fig. 27. In the figure solid and broken lines denote air temperature and dew point respectively and the height is indicated both in mb and meter.

From the figure it is considered that the height of cirrus observed at the stations is at the level indicated with arrows, i. e. 488-mb at Hamamatsu and 494-mb at Shionomisaki . The observed relative humidity at these levels is 38 and 49 % respectively. It is worthwhile that cirrus can exist even if the relative humidity is below 50 % as is verified in this example.

It should also be pointed out that partly cloudy extremely thin cirrus which can be observed by human eyes can not be recognized even in MSS picture which has extremely high resolution.

During the process of analysis it was pointed out by a few veteran pilots that the fan shaped cirrus visible in this picture often appears when a typhoon or severe tropical storm exists far to the south. Actually there was a severe tropical storm of 990-mb 1000 kms due south of Hamamatsu.

8.3 Radiation characteristics

Using the digital tape of LANDSAT the global albedo of the land surface and cirrus is computed and shown in Table 4.

Table 4 The global albedo computed from MSS digital data. (Unit: %)

Area		MSS Band				Total
		4	5	6	7	
Mountain area (D)	M.	9.6	5.9	15.7	26.8	15.7
	S.D.	1.6	0	5.3	10.1	
Cultivated area (To N of A)	M	15.5	12.4	19.6	26.8	19.4
	S.D.	1.4	1.7	2.8	5.5	
Urban area (A)	M	17.4	14.1	14.2	16.2	15.7
	S.D.	2.8	1.4	1.8	2.4	
Cirrus above sea (E)	M	16.0	10.7	9.3	9.4	11.4
	S.D.	1.4	1.4	1.1	1.3	
Lake Hamana (B)	M	9.6	5.9	3.9	2.8	5.5
	S.D.	0	0	0	0.9	
Ise Bay(C)	M	13.2	6.8	5.3	4.0	7.3
	S.D.	0.7	0	0	0.9	

M: Mean

S.D.: Standard Deviation

Note: The location of each area is indicated with letters.

25

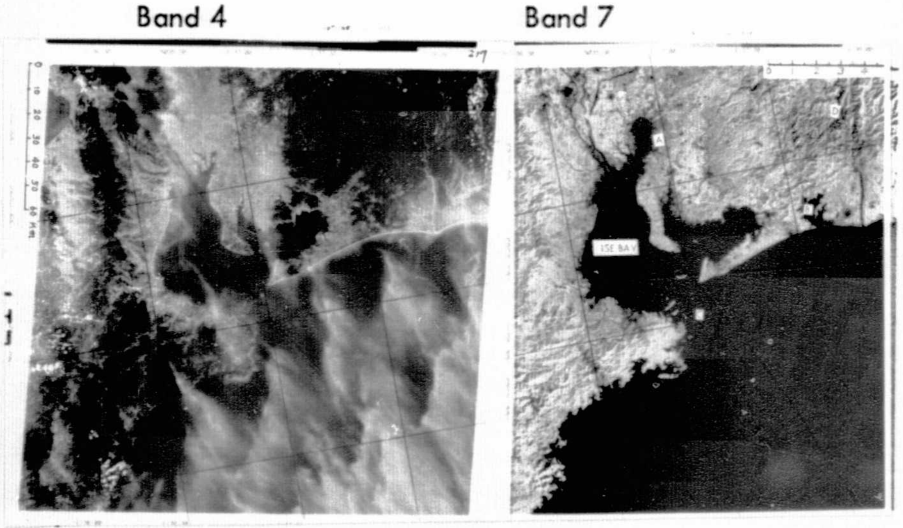

Fig. 25 Pictorial representation of LANDSAT MSS data 01 GMT Oct 5 1972.

26

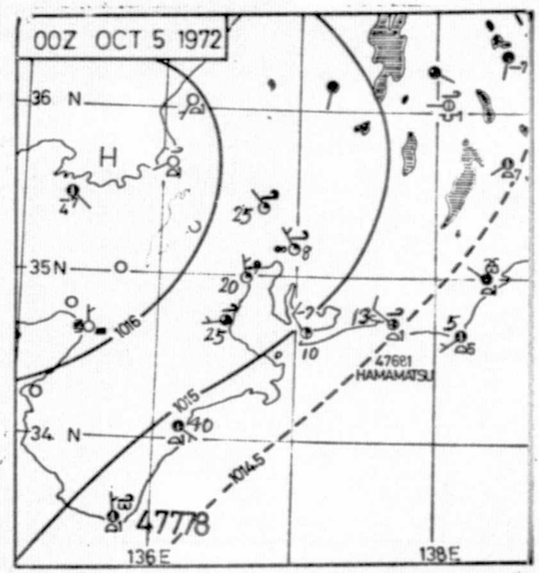

Fig. 26 Surface weather map showing cloud distribution and visibility in kms. 00 GMT Oct 5 1972.

27

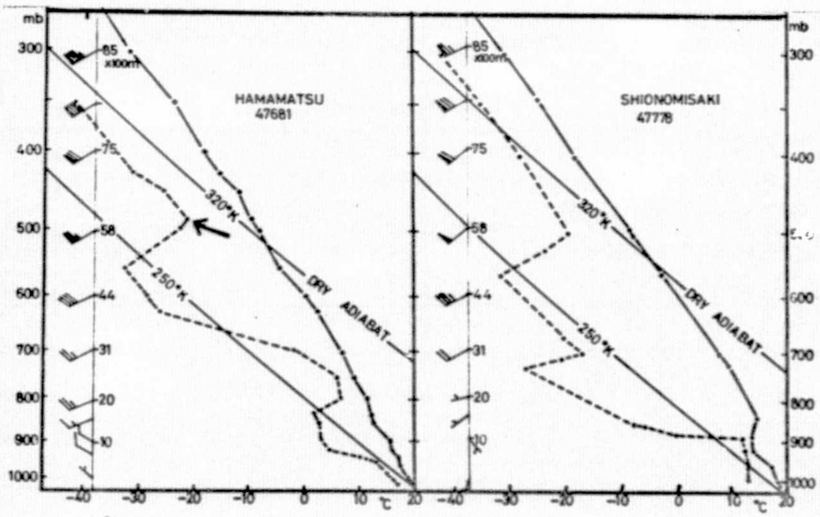

Fig. 27 Radio sounding at Hamamatsu and Shionomisaki plotted on an Emagram. Air temperature and dew points are shown in solid and broken lines. 00GMT Oct 5 1972.

In the table the value of Ise Bay is a little larger than that of Lake Hamana which is considered due to the effect of smog over the bay. It is interesting to compare the values of the urban area with those of mountainous area. In short wave spectrum (Band 4) the global albedo of the urban area is much larger than that of the mountainous area with thick vegetation while in the long wave spectrum(Band 7) the value is opposit, however in the range of whole spectrum of 0.5 - 1.1 um the balue of the both areas is equal in the value.

Cirrus shows the so called non-selective characteristics except Band 4. The large value in Band 4 is considered partly due to the effect of smog and partly due to the effect of scattering by air molecules and aerosols. Since the shorter the wave length the larger is scattering, the effect of scattering in the space is the largest in Band 4.

The large standard deviation of mountainous area in Band 7 is due to shadow effect. The largest global albedo in the whole spectral range is is found in the cultivated area. The sample of the cultivated area is located to the north of Nagoya and cover villeges and towns and small forests.

9. SEA FOG

Formation of dense sea fog takes place when a warm air over the land flow out over a cold sea surface. This type of fog is called sea fog and persists for long time and is a great problem for a navigation.

The sea off the east coast of Hokkaido is noted for frequent occurrence of dense sea fog. On July 16 1973 there was a dense sea fog over the sea to the east of Hokkaido as is shown in Fig. 28, surface weather map.

Fig. 29 is the color composit of LANDSAT MSS data showing the sea fog around Kunashiri Island (indicated with an arrow in the surface weather map. The smoke from the north-eastern tip of the island is the eruption just started a few days before. The clear cut boundary is the effect of the land of Hokkaido and Sakhalin.

The southern tip of Etorofu Island indicated by letter "A" in Fig. 28 is visible at the right middle edge of the picture. It is seen upwind side of the island is char terised with more dense sea fog. It is considered that fog area is due to the effect of

Microscopic analysis indicates very short wave motion exists, the wave length of which is approximately 1 km.

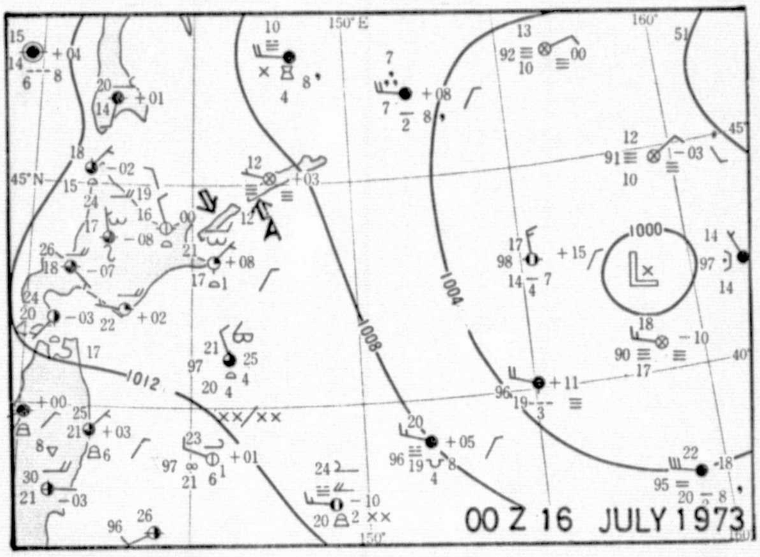

Fig. 28 Surface weather map at 00 Z 16 July 1973. Notice extensive sea fog over the ocean. The arrow indicates Island Kunashiri and the Island with A is Etorofu Island.

Fig. 29 Color composit of LANDSAT MSS data showing sea fog. Smoke denotes erution of Volcano Chacha. 01 GMT 16 July 1973.

CONCLUDING REMARK

The foregoing analyses lead to the following concluding remarks. LANDSAT data are extremely useful for the study of mesoscale phenomena. Some of ;the conclusions derived from low resolution meteorological satellite data must be modified to a certain extent.

Most of the so called longitudinal clouds which appear as continuous linear clouds are in reality composed of small transversal clouds. There are mountain waves of different wave length in a comparatively narrow area indicating complicated orographical effects on wind and temperature distribution or on both dynamical and static stability condition.

There is a particular shape of cirrus cloud suggestive of turbulence in the vicinity of CAT in the upper troposphere near jet stream level and its cold air side.

Thin cirrus of overcast condition can be distinguished by using MSS data, however extremely thin cirrus of partly cloudy condition can not be detected even in LANDSAT data. This fact presents a serious problem in the interpretation of satellite thermal infrared radiation data since they affect the value. MSS data can effectively used for the study of atmospheric radiation cinclusing the effects of smog and aerosols.

It is also found that LANDSAT data are one of the best at present to obtain snow cover area.

REFERENCES

Alaka, M A, 1960: The airflow over mountains. WMO Tech. Report 98, pp 132, WMO.

Asai, T., 1964: Photographic observation of clouds by aircraft during the snowfall period in the Hokuriku District. J. Meteor. Soc. Japan, 42, 186-190.

______, 1966: Cloud bands over the Japan Sea off the Hokuriku District during a cold air outbreak. Papers in Meteor. and Geophysics. Meteor. Res. Inst. Japan.

Bénard, H., 1900: Les tourbillons cellulaires dans une nappe liquide. Rev. gen. Sci. pur Appl., 11, 1309-1328.

______, 1928: Sur les tourbillons cellulaires, les tourbillons en bands, et la théorie de Rayleigh. Bull. Soc. Franç. Phys., 266, 112-115.

Döös, BO. R., 1962: A theoretical analysis of lee wave clouds observed by TIROS I. Tellus, 14, 303-309.

Foldvik, A., 1962: Two dimensional mountain wave - - A method for the rapid computation of lee wave lengths and vertical velocity. Quat. J. Roy. Meteor. Soc., 88, 271-285.

Fritz, S., 1965: The significance of mountain lee waves as seen from satellite pictures. J. Appl. Meteor., 4, 31 -37.

Ishihara, K., 1967: Estimation of snow cover depth and temperature based on topographical parameters.* Highways and Automobile, Vol. 6, No. 6.

Kuettner, J. P., 1971: Cloud bands in the earth's atmosphere. Tellus, 23, 404-426.

Kreuger, A. F. and S. Fritz, 1961: Cellular cloud pattern revealed by TIROS I., Tellus, 13, 1-7.

Priestrey, C. H. B.,1961: The width-height ratio of large convective cells., Tellus, 14, 123-124.

Tsuchiya, K., 1967: A satellite meteorological study of evaporation and cloud formation over the western Pacific under the influence of winter monsoon. J. Meteor. Soc. Japan, 45, 232-250.

__________, 1969: The morphology of winter monsoon clouds around Japan. Geoph. Magazine, 34, 427-445, Japan Meter. Agency.

__________, 1974: Cloud features associated with mesoscale phenomena during cold season as revealed by meteorological satellite pictures. Geoph. Mag.,39, 49-94.

__________,1974: Survey of meteorology from space.* Satellite pictures of Japan, 99-120, Asakura Pub. Co., Tokyo, Japan.

*: Original text in Japanese.